# Pupil optimization for after etch defectivity: what imaging metrics matter?

Frommhold, Andreas, Franke, Joern-Holger, Nafus, Kathleen, Rispens, Gijsbert, Maslow, Mark

Andreas Frommhold, Joern-Holger Franke, Kathleen Nafus, Gijsbert Rispens, Mark J. Maslow, "Pupil optimization for after etch defectivity: what imaging metrics matter?," Proc. SPIE 11854, International Conference on Extreme Ultraviolet Lithography 2021, 118540H (19 October 2021); doi: 10.1117/12.2600967

SPIE.

Event: SPIE Photomask Technology + EUV Lithography, 2021, Online Only

# Pupil optimization for after etch defectivity - what imaging metrics matter?

Andreas Frommhold*[a], Joern-Holger Franke[a], Kathleen Nafus[b], Gijsbert Rispens[c], Mark Maslow[c]
[a]imec, Kapeldreef 75, 3001 Leuven, Belgium
[b]Tokyo Electron Kyushu Ltd., 1-1 Fukuhara, Koshi City, Kumamoto 861-1116, Japan
[c]ASML Netherlands B.V., De Run 6501, 5504 DR Veldhoven, The Netherlands

## ABSTRACT

A series of experiments was conducted to study how defectivity depends on NILS, aerial image intensity and depth-of-focus. Three sets of illuminations were designed to vary only one of these parameters while keeping the others constant for a 48 nm pitch orthogonal contact hole array. The focus was on the after etch defectivity, for which two different etch processes were studied. Both on-wafer LCDU and defectivity for the two etch processes were correlated to the different illumination settings. In summary, we found that defect levels correlate best with the maximum intensity for missing holes and minimum intensity for merging holes. Depth-of-focus appears to have little or no impact on defectivity for the nominal focus condition.

**Keywords:** EUV lithography, imaging, defectivity, plasma etch

## 1. INTRODUCTION

In EUV lithography scaling is limited by defectivity. The main driver of this is stochastic variability. It can be reduced by optimizing the aerial image. Typically, this means increasing the normalized image log slope (NILS). However, it has been suggested that intensity-based metrics are a better predictor for defectivity[1,2] (Fig. 1). Also, depth-of-focus could conceivably play a role as it leads to varying CD and NILS through the resist film. Understanding the relative importance of these parameters is of paramount importance to predict the defectivity expected for high-NA imaging where NILS and intensity are improved but depth-of-focus deteriorates.

To understand how defectivity depends on NILS, aerial image intensity and depth-of-focus, three sets of illuminations were designed to vary only one of these parameters while keeping the others constant. This was possible for depth-of-focus, while intensity and NILS are generally strongly correlated. At the given pitch of 48nm contact hole orthogonal arrays, it was possible to increase peak intensity at constant NILS and depth-of-focus by first increasing the number of diffraction orders captured and then increasing fading until NILS is matched.

Since After Development Inspection (ADI) metrology does not always provide the full view on defectivity and improvements to the illumination in ADI are sometimes seen to not transfer well to After Etch Inspection (AEI), the focus here was on the after etch defectivity. Using a contact hole defectivity vehicle and pattern transfer enabled optical defect inspection. To ensure that the pupil optimization is reliably found back in AEI, two different etch processes are studied. In this way it is also verified whether source optimization provides additional benefits when using an advanced etch process or whether different etch processes require a different aerial image. On-wafer LCDU and defectivity for both etch processes were correlated to the different illumination settings.

## 2. SOURCE OPTIMIZATION

The goal of the experiment was to disentangle the influence of depth-of-focus, exposure latitude (or NILS) and the maximum intensity of an aerial image on the LCDU and AEI defectivity. Therefore, the aim was to design sources that vary only one of these parameters at a time while keeping the others constant. Overall, seven illuminations were constructed belonging to three systematic variations. The blue series varied depth-of-focus at constant peak NILS and maximum intensity. The orange/red series increased both maximum intensity and peak NILS at depth-of-focus values covered by the

*andreas.frommhold@imec.be

International Conference on Extreme Ultraviolet Lithography 2021, edited by Kurt G. Ronse, Patrick P. Naulleau, Paolo A. Gargini, Toshiro Itani, Eric Hendrickx, Proc. of SPIE Vol. 11854, 118540H · © 2021 SPIE · CCC code: 0277-786X/21/$21 · doi: 10.1117/12.2600967

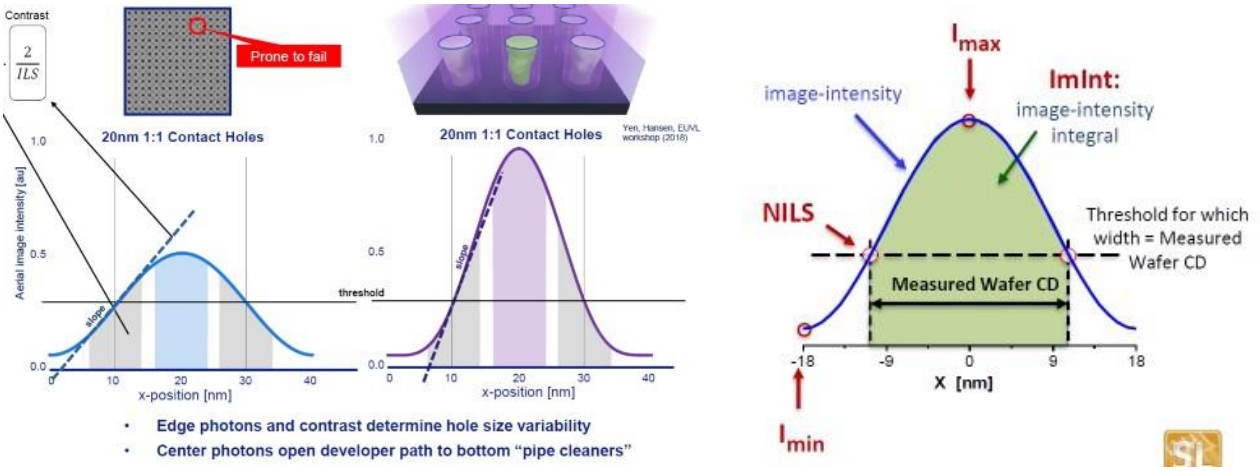


*Figure 1: Examples from literature highlighting the role of aerial image intensity in defectivity[1,2]*

blue series. The last variation was two pupils that differentiate peak NILS and maximum intensity (green series).

Fig. 2a shows the number of diffraction orders that are captured through different pupil locations for regular contact holes at pitch 48. To avoid complex scanner setup and asymmetric aerial images, 4-fold symmetric illuminations were used throughout. Depending on where the pixels are placed, different diffraction orders are captured leading to different aerial images. Putting a source pixel in the 4-beam region gives the diffraction pattern shown in Fig. 2b. The aerial image that results from these 4 diffraction orders will be dominated by spatial frequencies corresponding to the pitch itself (plus some higher frequency diagonal components). If a pixel is in the central region, the numerical aperture captures the diffraction orders as shown in Fig 2c. In this case, the presence of +/-1st orders will lead to spatial frequencies in the aerial image of twice the pitch, i.e., corresponding to pitch 24. This means that this aerial image will be sharper at small CD and will have higher maximum intensity in the center of the aerial image as well as higher image-log-slope at small CD. These two different aerial images form the building blocks of the illumination variations.

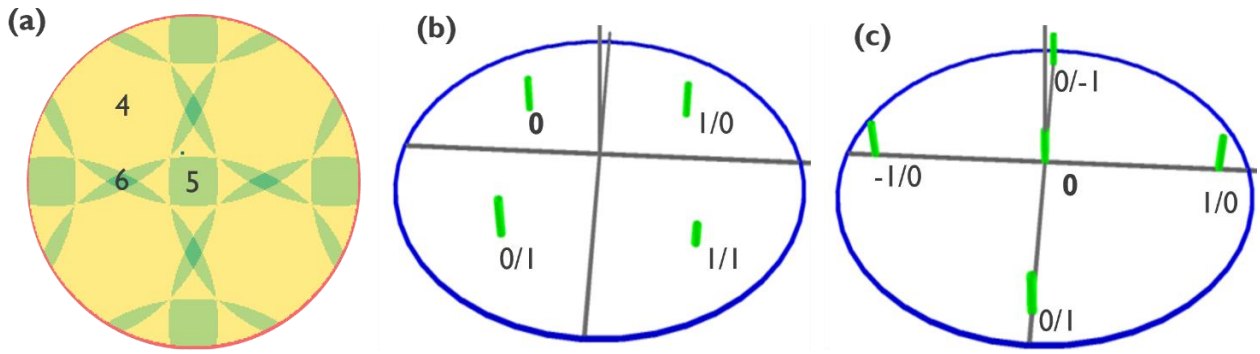


*Figure 2: (a) Pupil map counting the number of captured diffraction orders. The specific diffraction orders captured are shown for two cases, corresponding to 4-beam imaging (b) and 5-beam imaging from the central region (c). 0 denotes the 0th diffraction order, which corresponds to the position of the source pixel in (a)*

After selecting which diffraction orders will form the individual aerial image, the exact position of the pixel within the region for which the desired orders are captured is selected (e.g., the yellow region containing the number "4" in Fig. 2a which is delineated by the green regions). This position will control the through-focus behavior of the aerial image.

To construct pupils at constant peak NILS and variable depth-of-focus, the position on the 4-beam imaging pole is varied. An important effect to consider is that a relative phase offset of the 0th order against the 1st orders coming from M3D phase effects will lead to aerial image offsets of each source point at nominal focus. Combining multiple pixels from the four poles of a 4-fold symmetric source (i.e., a quasar source) will average out these offsets and convert them into NILS loss ("fading"). This is a two-dimensional equivalent of the effect observed for dense L/S where opposite poles show image offsets of opposite sign at nominal focus[3].

Placing source points not at telecentric sigma (the point for which the diffraction pattern is symmetric around the optical axis), but at a distance in the pupil plane, the aerial image becomes non-telecentric. By displacing the source points along the diagonal of the plane, the non-telecentricity can be used to compensate the center offset at a defocus position. This would reduce NILS loss but lead to a best focus offset from nominal focus and drive down depth-of-focus as the images coming from different poles disperse more quickly through focus. Choosing pixels for which the diffraction pattern becomes symmetric (pixels at "telecentric sigma") will maximize depth-of-focus, while pixels near the edge of the yellow region will minimize it.

Keeping the NILS at best focus constant but decreasing depth-of-focus is achieved by symmetrizing the pupils around the telecentric sigma. The larger the distance to telecentric sigma, the higher the non-telecentricity of the aerial image coming from each pole. By pairing each non-telecentric pixel with its opposite (by constructing sources that are point symmetric around telecentric sigma) they will still loose depth-of-focus, but not gain NILS in out-of-focus conditions any longer. A source series starting with a dot at telecentric sigma and going stepwise towards a ring at the outer edge of the pupil will have constant NILS (and max. intensity) at decreasing depth-of-focus. This is the blue source or NFC series. NFC or NILS(focus) curvature is the quadratic term of the NILS(focus) parabola and describes how fast NILS degrades in defocus. To illustrate NFC, Table 1 summarizes the values of the NFC pupils together with the associated NDOF (DoF over which the NILS is above 2) from aerial image simulation and CD-based DoF measured on the wafers. Bear in mind that the CD-based DoF is highly dependent to the chosen CD and as such susceptible to metrology offsets as well as Bossung curvature scaling effects from the resist. As we do not have a reliable "aerial image to wafer matching" methodology the relation between NFC and CD-DoF is only tentative and solely shown for illustrative purposes.

*Table 1 Summary of aerial image metrics for the blue source or NFC series (*from aerial image simulation; **highly sensitive to chosen CD and as such susceptive to metrology offset & resist scaling effects)*

| Pupils | peak NILS* | NFC/NILS* | NDOF (NILS>2)* | CD-DOF@10%EL** |
|---|---|---|---|---|
| 1 | 2.713 | -46.40 | 150 nm | 159 nm |
| 2 | 2.726 | -31.65 | 186 nm | 239 nm |
| 3 | 2.711 | -7.26 | >300 nm | 398 nm |

The second series consists of sources that optimize peak NILS and maximum intensity by making use of the higher beam count regions of the pupil plane. Here the peak NILS and maximum intensity are very closely correlating and hard to disentangle. (red/orange sources). The only way to do this is to mix sources with higher spatial frequencies with sources with lower spatial frequencies. This would mean mixing 5- or 6-beam imaging into a 4-beam imaging source. Doing so drives up both peak NILS and maximum intensity. To differentiate maximum intensity from peak NILS sources are constructed from different spatial frequencies that nevertheless obtain the same peak NILS. A high spatial frequency source will give high maximum intensity, but it can lose some NILS due to fading. Matching this NILS with a source made entirely from low spatial frequencies but with significantly reduced fading due to source points being offset from telecentric sigma (to partially compensate fading out-of-focus) leads to the green pupil series.

Interestingly, this fading-reduced low-frequency source also results in far lower minimum intensity than all other sources. Minimum intensity is therefore driven mostly by fading and not high spatial frequencies. This is an interesting fact to keep in mind when thinking about better image contrast afforded by high-NA to reduce defectivity: for initial, non-critical pitches using high-NA, minimum intensity will be higher than when imaging with well optimized pupils with low-NA.

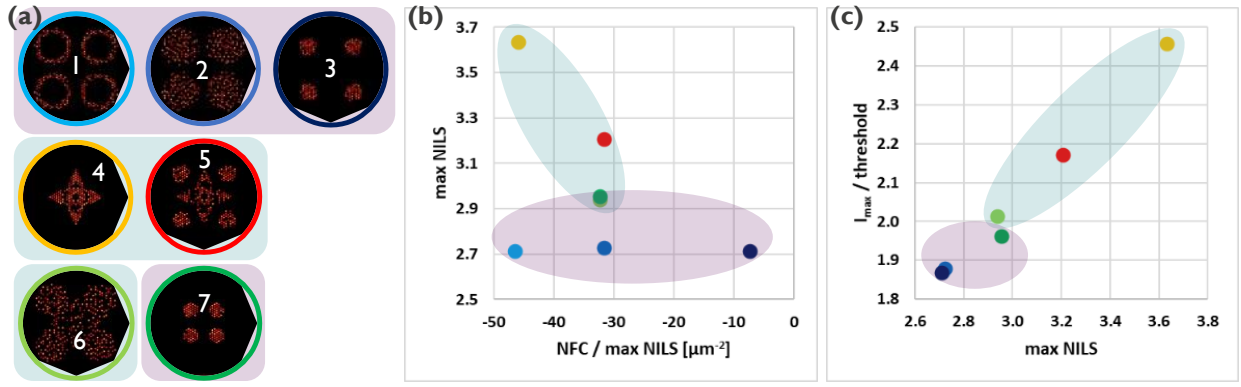


*Figure 3: (a) Different sources constructed. Sources 1-3 vary depth-of-focus at constant peak NILS/max. intensity, sources 4/5 maximize peak NILS and max. intensity, sources 6/7 differentiates peak NILS and max. intensity. (b) max. NILS and NILS(focus) curvature of all sources. (c) max. NILS vs. max. intensity (normalized to threshold-to-CD24).*

## 3. EXPERIMENTAL CONDITIONS

Tools and metrology are summarized in Table 2. In this study, 24 nm 1:1 dense contact hole patterns were printed with EUV lithography using a TWINSCAN NXE:3400B scanner (N.A.: 0.33). A tri-layer stack consisting of a spin-on-carbon (SOC) under-layer, a spin-on glass (SOG) middle layer and a chemically amplified photoresist layer was coated and developed using TEL CLEAN TRACK™ LITHIUS Pro™ Z coater and developer. Patterns were transferred to a SiN layer with Tactras™ Vigus™. Two etch processes were used in this study. The first etching process used is a standard process based on lean chemistries to transfer the holes vertically into the underlying layers. A second process using a descum step combined to a cycling between deposition and etching was also used. This kind of process helps decreasing defectivity and corrects CD variations thanks to micro-loading effects.CD measurements and the defect inspections were performed at After Development Inspection (ADI) and After Etching Inspection (AEI).

*Table 2 Tool and metrology*

| Process | Tool | Company |
|---|---|---|
| Exposure | TWINSCAN NXE : 3400 | ASML |
| Coater and developer | CLEAN TRACK™ LITHIUS Pro ™ Z | Tokyo Electron Ltd. |
| Etching | Tactras ™ Vigus ™ | Tokyo Electron Ltd. |
| Defect Inspection | KLA2935 | KLA |
| Defect review | EDR7380™ | KLA |
| CD measurement | CG6300 | Hitachi |

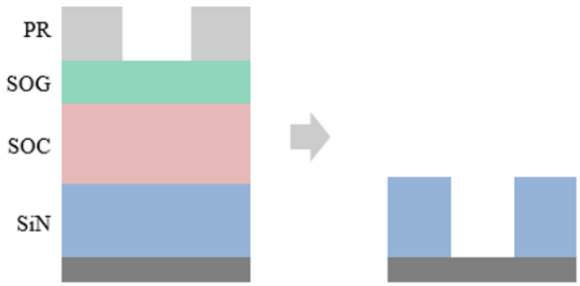


*Figure 4: Stack at the inspection steps (left) ADI and (right) SiN open*

## 4. RESULTS & DISCUSSION

First, the LCDU for the different illuminations was examined, specifically the decomposition of LCDU into its stochastic and systematic components. The decomposition was performed as described elsewhere[4]. LCDU provides an experimental measure of the NILS and as such is also linked to defectivity[5]. While the stochastic component characterizes the randomness in every exposure, the systematic part is part of every die and mainly attributed to the mask and reproducible effects in the scanner. The stochastic part follows expectations as it correlates well with the maximum NILS of the pupils (Fig. 5). While the absolute values differ for ADI and the two etch processes, the trend through the pupils is clearly visible for all three cases. For the new etch process it is slightly noisier, but the correlation is still high. Aerial image simulation was sufficient to predict the stochastic LCDU trend, no resist blur, mean-to-target for the mask making process or metrology offset had to be applied. One point of attention is the slight difference in stochastic LCDU visible for all three cases in the green series, which by design shares the same NILS and NFC. But the pupil with the higher maximum intensity has a slightly worse value. This could already indicate the relative importance of aerial image intensity.

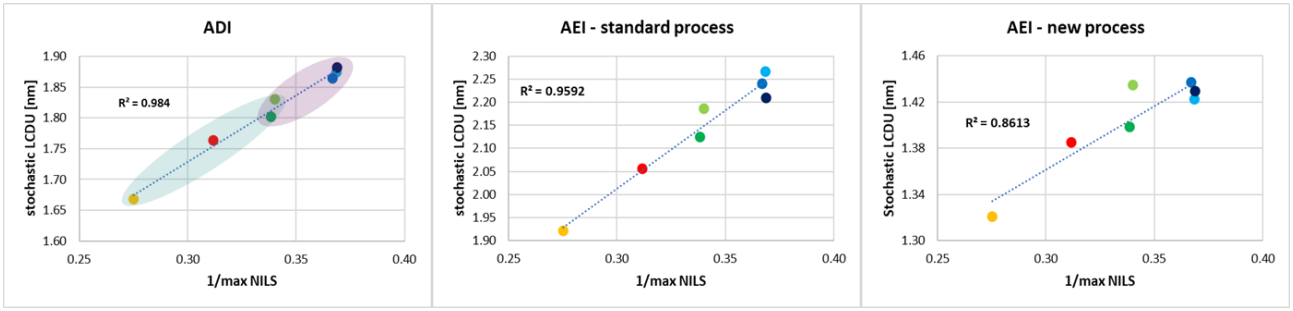


*Figure 5 Correlation of stochastic LCDU to maximum NILS after litho and after the two etch processes*

The systematic LCDU component is expected to follow the mask error enhancement factor (MEEF). MEEF characterizes the translation of the mask pattern variability onto the wafer through the used illumination. In general, the systematic LCDU also follows the simulated MEEF here, except for one clear outlier - the low fading inner sigma illumination (pupil 7) has a low MEEF but shows an excursion in the systematics in opposition to pupil 6 (figure 6). We have encountered this behaviour also in other cases and are currently working on understanding this behaviour. It appears to be linked to the use of inner sigma illumination pixels. Also, the small spread in the blue series is potentially linked to the same issue as the pupils use different sigma settings. We note that etch effectively reduces this spread.

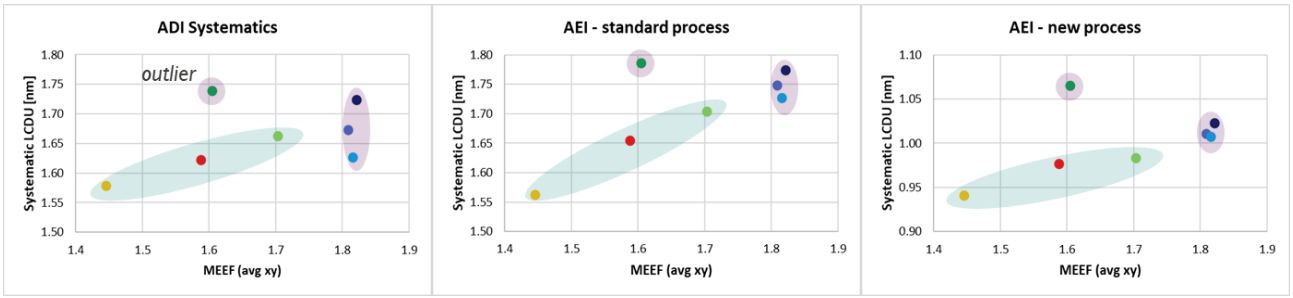


*Figure 6 Correlation of systematic LCDU with simulated MEEF after litho and after the two etch processes*

A first assessment of the optical inspection defectivity results was done with a low sensitivity setting on FEM wafers. A clear ordering of the defect rates with respect to the used illumination was found at the small and large CD side where the missing and merging contacts are found (Fig. 7). This correlates well to the ranking of the pupils in terms of the maximum intensity in the centre of the aerial image for the missing contacts and the minimum intensity in the dark part of the aerial image, where due to the diffraction there is still a bit of light. It is important to assess the minimum and maximum in relation to the threshold of the print CD. The intensity plots are further normalized to the largest value to show the relative differences between the pupils. At the small CD side, the pupil with the highest maximum intensity has the lowest defect level. On the large CD side, where the minimum intensity is highest the largest defectivity is found. The ranking of the pupils with regards to defectivity is then followed well by the maximum and minimum intensity over the threshold. Note

that while the yellow pupil leads the performance on missing failures, it also has the worst defectivity for merging holes due to having both the highest maximum and minimum intensity.

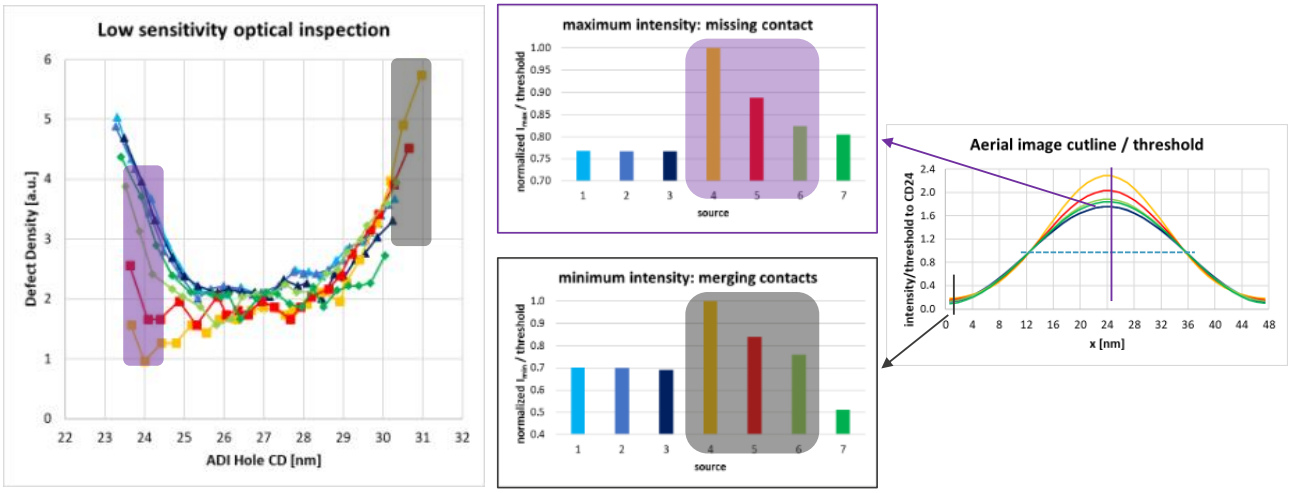


*Figure 7 Low sensitivity optical defect inspection on FEM wafers and corresponding aerial image intensities*

After optimization of the experimental conditions, it was possible to increase the sensitivity of the optical inspection to a medium setting for the standard etch process to differentiate further the defectivity performance between the illuminations. Plotting the aerial image log slope (ILS), two distinct regimes can be distinguished (Fig. 8 right). For small CDs, the pupils with the higher beam counts have higher ILS leading to the defect cliff for the missing holes being pushed out (Fig.8 left). The defect floor also scales with the ILS of the pupils and there is a clear ranking in terms of the defect density. But with increasing CD at a certain point the 4-beam illuminations have a higher ILS and the ranking of the pupils for the merging failures reverses. The pupil performance is hence strongly dependent on the CD. In addition, there is some differentiation in the blue series that cannot be explained by the ILS because of the matching. Instead, the NFC appears to have a small impact on the defect floor, with the pupil of lowest NFC also having a lower defectivity.

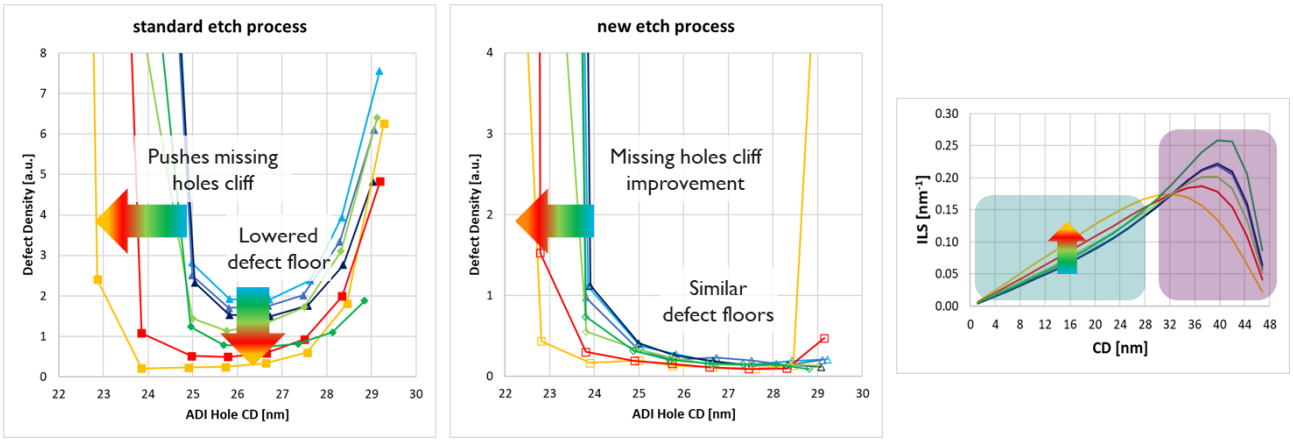


*Figure 8 Optical defect inspection for (left) standard etch with medium sensitivity, (middle) new etch process with high sensitivity setting and (right) aerial image log slope for the illuminations versus print CD*

The new etch process is very effective in reducing defectivity so that the inspection sensitivity was further increased. A similar picture of higher ILS pushing out the defect cliffs and the reversal in the ranking of the pupils was found (Fig. 8 middle). From this we conclude that the benefits of the pupil optimization transferred well from ADI to AEI. In the defect floor the new etch reduces the variability and brings down the number of defects to such an extent that it becomes difficult to distinguish the pupils as they all show a similar floor including the series on NFC-dependence.

In summary, defects correlate well with the peak intensity in the aerial image in the centre of the feature and the space between the features respectively. At the same time a higher NILS effectively pushes out the defect cliffs. To answer the

final question, which metrics matters the most, the two metrics must be disentangled. Pupils 6 and 7 were designed to this purpose. Focusing on those data points in the correlation plots (Fig. 9) it is observed in the correlation of the defect counts versus the NILS that there is a difference in the defect levels which the NILS cannot distinguish because the pupils were designed to the have the same NILS. Hence, they fall on the same line on the horizontal axis. Also, in the defect correlation to stochastic LCDU the higher maximum intensity pupil is lower in defectivity despite being penalized by a higher stochastic LCDU value. On the other hand, correlating the defect rates to the maximum intensity the pupils are ordered correctly and exhibit an almost perfectly linear trend. From this it is concluded that the intensity over the threshold best predicts the defectivity and is deemed to most critical metric.

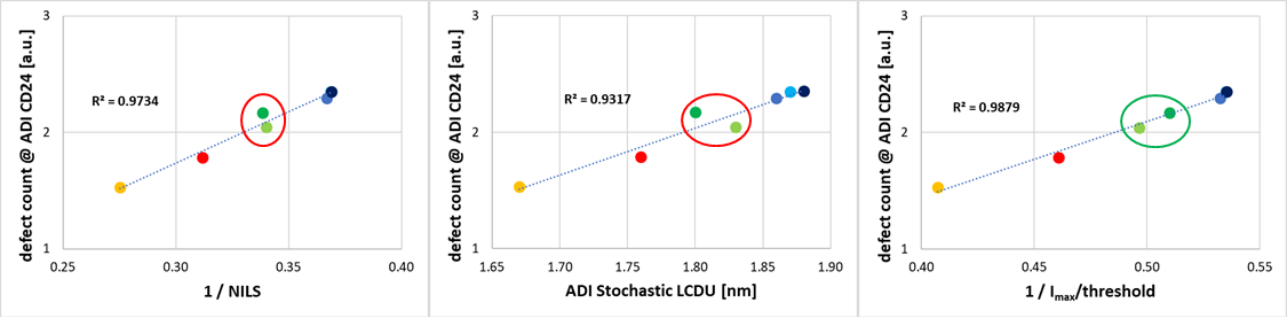


*Figure 9 Correlation of defect rates to (left) NILS, (middle) stochastic LCDU and (right) maximum aerial intensity over threshold*

## 5. CONCLUSIONS

The LCDU and defectivity of a set of designed pupils was studied to clarify which imaging metric is the most important. It was found that the stochastic LCDU is well predicted by the NILS while the systematic LCDU is generally predicted by the MEEF. Some irregular behavior in the systematics was observed, which appears to be linked to an unknown effect for inner sigma pupils. No evidence for NFC-driven degradation of the LCDU at nominal condition was seen, at least for the range tested here.

In terms of defectivity the defect levels correlated best with the maximum intensity over threshold for missing holes and minimum intensity over threshold for merging holes (Fig. 10). By improving NILS by 35 percent and the maximum intensity by 32 percent the defect levels could be reduced by two orders of magnitude. Depth-of-focus appears to have little or no impact on defectivity for the nominal focus condition (etch process dependent). This would be beneficial for High-NA. However, caution must be applied as Depth-of-focus will be more limited in 0.55NA than what can be sampled in 0.33NA. The improved maximum intensity and NILS in High-NA would lead to gains in LCDU and less missing holes. However, increasing the number of diffraction orders captured also results in higher minimum intensity and more merging holes. This effect is linked to phase differences between diffraction orders which could conceivably be mitigated by transitioning to a different mask stack.

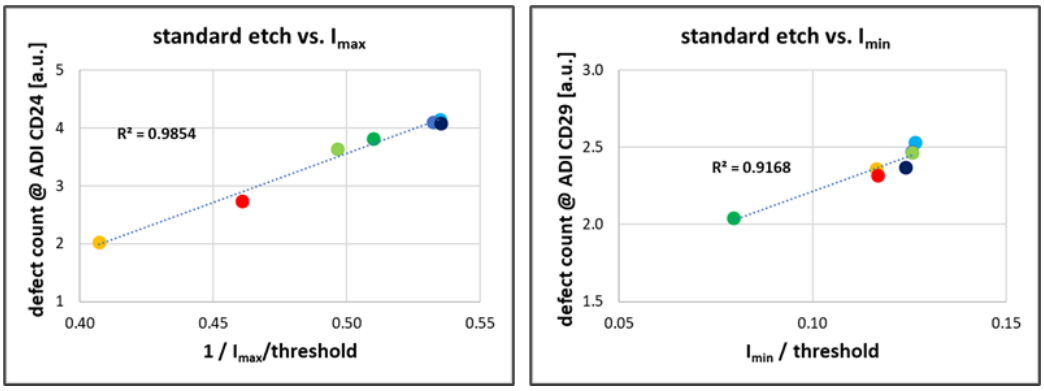


*Figure 10 Correlation of defect rates with (left) the inverse of the aerial image intensity maximum over threshold and (right) the intensity minimum over threshold*

In the end, based on the obtained results, the metrics are ranked in terms of their impact on defectivity in the following order: (1.) minimum & maximum intensity over threshold, (2.) NILS and (3.) NFC. It should be noted that the intensity and the NILS are often strongly coupled and increasing one will also increase the other. Furthermore, driving up the maximum intensity will also increase the minimum intensity if fading is not compensated. Each of the metrics impacts a different aspect of the contact hole feature. The intensities act predominantly on the center of the contact hole and the space between the contacts. The results seem to support the hypothesis that the increased number of photons in the center help opening a developer path to the bottom of the feature, while reduced photon counts prevent resist lost in the space between features. NILS affects mostly the circumference of the holes where the edge is formed. A low NILS would lead to strong variability of the contact shape that in turn could promote the formation of defects. NFC can be pictured as NILS loss through the resist stack. Thick resists are typically used for the patterning of contact holes. Assume the best focus for the aerial image is positioned at the top of the hole, which is reasonable as targeting the process is performed via top-down CDSEM inspection. Then if NFC is high, NILS drops considerably over the depth of the resist profile leading to tapered side walls and possible scum formation at the bottom. Since after etch inspection is performed, the etch process potentially alleviates this by breaking through the scum and straightening the sidewalls so that the impact of NFC appears small. Ultimately it would be interesting to repeat this study once high-NA imaging becomes experimentally available to verify whether the effect of the strongly increased NFC becomes more pronounced.

## ACKNOWLEDGEMENTS

The authors are greatly indebted to Arnaud Dauendorffer from Tokyo Electron Ltd. for providing all the defect inspection and metrology results as well as discussion thereof.

## REFERENCES

[1] Van Schoot, J., Lok, S., van Setten, E., et al., “High-NA EUV lithography exposure tool: advantages and program progress,” Proc. SPIE 11517, 1151712 (2021).

[2] De Bisschop, P., Hendrickx, E., “On the dependencies of the stochastic patterning-failure cliffs in EUVL lithography,” Proc. SPIE 11323, 113230J (2020).

[3] Franke, J.-H., Bekaert, J., Blanco, V., et al., “Improving exposure latitudes and aligning best focus through pitch by curing M3D phase effects with controlled aberrations,” Proc. SPIE 11147, 111470E (2019).

[4] Van Look, L., Bekaert, J., Frommhold, A., et al., “Optimization and stability of CD variability in pitch 40 nm contact holes on NXE:3300,” Proc. SPIE 10809, 108090M (2018).

[5] Maslow, M.J., Yaegashi, H., Frommhold, A., et al., “Impact of local variability on defect-aware process windows,” Proc. SPIE 10957, 109570H (2019).